Modification of cavity ring-up spectroscopy

Meng-Chong Shen, Ming-Yong Ye,* and Xiu-Min Lin
Fujian Provincial Key Laboratory of Quantum Manipulation and New Energy Materials, College of Physics and Energy, Fujian Normal University, Fuzhou 350117, China
and Fujian Provincial Collaborative Innovation Center for Advanced High-Field Superconducting Materials and Engineering, Fuzhou 350117, China

(Received 10 December 2021; revised 11 February 2022; accepted 25 February 2022; published 14 March 2022)

Cavity ring-up spectroscopy (CRUS) can be used to sense ultrafast phenomena with a timescale of a nanosecond and it has been experimentally demonstrated in whispering-gallery-mode (WGM) microresonators. Here, we present a modification of CRUS in which the intensity of the monochromatic laser used to excite a WGM microresonator is changed from one nonzero value to another nonzero value within a very short time. The modification doubles the sampling rate of CRUS at almost no cost, which is important in ultrafast sensing. We first give a theory of the modified CRUS and then show its experimental observation. The obtained results make the developing CRUS more complete.

DOI: 10.1103/PhysRevA.105.033509

I. INTRODUCTION

Optical whispering gallery modes (WGMs) are usually of very high-quality factors and extremely small mode volumes. These features enable WGM microresonators to become good platforms for studying interactions between light and matter [1–18]. Sensing is one of the most important applications of WGM microresonators [19–21]. In particular, they can be used to detect single nanoparticles and viruses [22]. The sensing mechanism of WGM microresonators is usually related to some change of the steady-state transmission spectrum of the system, which can be obtained by using a continuous laser to scan the microresonators at a slow speed with a fiber taper as a light coupler [23,24]. The main changes of the steady-state transmission spectrum used for WGM sensing are a mode shift [25], splitting [26], and broadening [27]. However, the sensors based on these mechanisms can be only used to detect parameters changed on a timescale of milliseconds due to the slow scanning speed of the laser. The sensing of ultrafast phenomena by WGM microresonators needs a new sensing mechanism.

Recently, cavity ring-up spectroscopy (CRUS) of WGM microresonators is demonstrated to have the ability to sense ultrafast phenomena with nanosecond timescales [28–30]. Interference is important in CRUS and other related ringing phenomena in WGM microresonators [31–33]. To obtain CRUS, a far-detuned laser is abruptly turned on to excite a microresonator [28], which is different from the ordinary cavity ring-down spectroscopy (CRDS) where a laser exciting a microresonator is abruptly turned off [34]. In CRUS, although there is a large detuning between the laser frequency and the resonant frequency of the microresonator, some light can still be coupled into the microresonator due to frequency broadening caused by turning on the laser abruptly. The light into the microresonator will be coupled back into the fiber taper to interfere with the transmitted light, which results in CRUS containing information on both the frequency and decay rate of the microresonator. This feature of CRUS is an improvement compared to the ordinary CRDS [28,35].

In the original CRUS, the intensity of the monochromatic laser used to excite microresonator is changed from zero to nonzero within a very short time [28]. Here, we consider the modified CRUS where the intensity of the monochromatic laser is changed from one nonzero value to another nonzero value within a very short time. In the case where the initial intensity of the laser is much smaller than the final intensity, the modified CRUS will be similar to the original CRUS. In the case where the initial intensity of the laser is much larger than the final intensity, the modified CRUS will be similar to CRDS. The modified CRUS in both cases contains information on the frequency and decay rate of the microresonator and thus can be used in ultrafast sensing. Experimentally, the intensity of the laser is switched between a small value and a large value periodically. Therefore, in one period two modified CRUS can be obtained (see Fig. 5 below). However, in the original CRUS experiment the intensity of the laser is switched between zero and a nonzero value periodically and only one CRUS can be obtained in one period [28]. So in our modified CRUS the sampling rate is doubled compared to the original CRUS, which is important in ultrafast sensing.

In the following we first give the theory of the modified CRUS, and then present our experimental studies.

II. THEORY OF MODIFIED CRUS

A. Modified CRUS without modal coupling

Figure 1(a) shows the basic theoretical model where a fiber taper is used to couple a specially modulated laser into and out of a WGM microresonator. The counterclockwise (CCW) mode E_1 is excited by the input field E_{in} in the fiber taper. The

*Corresponding author: myye@fjnu.edu.cn

 ©2022 American Physical Society

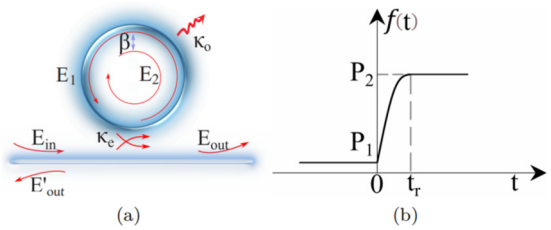

FIG. 1. (a) Schematic diagram of a WGM microresonator coupled to a fiber taper. (b) A steplike modulation function.

evolution of E_1 satisfies the following equation [36],

$$\frac{dE_1(t)}{dt} = (-j\omega_c - \kappa)E_1(t) + \sqrt{2\kappa_e}E_{\text{in}}(t), \tag{1}$$

where $j = \sqrt{-1}$, ω_c is the resonant angular frequency of the CCW mode E_1, κ_e and κ_o represent its external and intrinsic loss rates, and $\kappa = \kappa_e + \kappa_o$ is the total loss rate. We note that there is a degenerate clockwise (CW) mode E_2 corresponding to the CCW mode E_1 and usually there is a coupling between them. Here, the coupling strength between E_1 and E_2 is assumed to be zero, and the nonzero case will be discussed in a later section.

In Eq. (1), the input field $E_{\text{in}}(t)$ is a modulated monochromatic laser with the expression

$$E_{\text{in}}(t) = f(t)se^{-j\omega_l t}, \tag{2}$$

where s is the amplitude of the monochromatic laser, ω_l is the angular frequency of the monochromatic laser, and $f(t)$ is a steplike modulation function displayed in Fig. 1(b). The value of function $f(t)$ is P_1 when $t \leqslant 0$, and it changes abruptly to a stable value P_2 within a very short time t_r. What we are interested in is the output $E_{\text{out}}(t)$ of the fiber taper when $t > t_r$, which can be expressed as

$$E_{\text{out}}(t) = -E_{\text{in}}(t) + \sqrt{2\kappa_e}E_1(t). \tag{3}$$

When $P_1 = 0$ and $P_2 > 0$, the intensity $|E_{\text{out}}(t)|^2$ describes CRUS. When $P_1 > 0$ and $P_2 = 0$, the intensity $|E_{\text{out}}(t)|^2$ describes CRDS. In the following we assume there are both $P_1 > 0$ and $P_2 > 0$, which is a modification of CRUS.

We first show how $E_1(t)$ depends on the modulation function $f(t)$. Suppose

$$E_1(t) = h(t)se^{-j\omega_l t}\sqrt{2\kappa_e}, \tag{4}$$

then from Eq. (1) we can obtain

$$\frac{dh(t)}{dt} = (j\delta - \kappa)h(t) + f(t), \tag{5}$$

where $\delta = \omega_l - \omega_c$. Using method of the variation of constants, the above equation will lead to

$$h(t) = e^{(j\delta-\kappa)t}\int_{-\infty}^{t} f(t')e^{(-j\delta+\kappa)t'}dt', \quad t > t_r, \tag{6}$$

$$= \frac{P_2}{-j\delta+\kappa}[1 - e^{(j\delta-\kappa)(t-t_r)}\alpha], \quad t > t_r, \tag{7}$$

where

$$\alpha = \frac{1}{P_2}\int_0^{t_r}\frac{df(t')}{dt'}e^{(-j\delta+\kappa)(t'-t_r)}dt'. \tag{8}$$

In the above from Eq. (6) to (7) we have used the method of integrating by parts and the facts that $\frac{df(t)}{dt} = 0$ when $t < 0$ and $t > t_r$, and $f(t) = P_2$ when $t > t_r$. Now we can see clearly how $E_1(t)$ depends on the modulation function $f(t)$ through the parameter α, i.e.,

$$E_1(t) = \frac{\sqrt{2\kappa_e}}{-j\delta+\kappa}[1 - e^{(j\delta-\kappa)(t-t_r)}\alpha]E_{\text{in}}(t), \quad t > t_r, \tag{9}$$

which combined with Eq. (3) gives the dependence of $E_{\text{out}}(t)$ on the parameter α, i.e., for $t > t_r$ there is

$$E_{\text{out}}(t) = \left[\frac{j\delta + \kappa_e - \kappa_o}{2\kappa_e} - e^{(j\delta-\kappa)(t-t_r)}\alpha\right]\frac{2\kappa_e E_{\text{in}}(t)}{-j\delta+\kappa}. \tag{10}$$

Define the normalized transmission of the output of the fiber taper as

$$T(t) = \frac{|E_{\text{out}}(t)|^2}{\lim_{t\to\infty}|E_{\text{out}}(t)|^2}, \tag{11}$$

then from Eq. (10) it can be obtained that

$$T(t) = \left|1 - e^{(j\delta-\kappa)(t-t_r)}\frac{2\kappa_e\alpha}{j\delta+\kappa_e-\kappa_o}\right|^2, \quad t > t_r. \tag{12}$$

This is an exact expression for the normalized transmission $T(t)$, which describes the interference of two terms and the second term has the frequency δ and decay rate κ. The modulation function $f(t)$ can affect the amplitude of the second term of $T(t)$ in Eq. (12) through parameter α that will be discussed in the next section.

The expression of $E_{\text{out}}(t)$ in Eq. (10) is obtained by assuming there are both $P_1 > 0$ and $P_2 > 0$, but it is obviously applicable for the original CRUS, i.e., $P_1 = 0$. We note that it is also applicable for CRDS, i.e., $P_2 = 0$. This is because when P_2 approaches zero, although the value of α in Eq. (8) will approach infinity and the value of $E_{\text{in}}(t)$ in Eq. (10) will approach zero for $t > t_r$, their product $\alpha E_{\text{in}}(t)$ in Eq. (10) will approach a finite value. So the expression of $E_{\text{out}}(t)$ in Eq. (10) is a universal result that connects the original CRUS and the seemingly different CRDS.

B. Modulation function $f(t)$ and parameter α

If the time t_r for the modulation function $f(t)$ changing from P_1 to P_2 is so small that there are $|\delta t_r| \ll 1$ and $\kappa t_r \ll 1$, it can be obtained from the definition of α in Eq. (8) that

$$\alpha \approx \frac{1}{P_2}\int_0^{t_r}\frac{df(t')}{dt'}dt' = 1 - \frac{P_1}{P_2}. \tag{13}$$

This result means that the shape of the modulation function $f(t)$ from 0 to t_r in the modified CRUS is not important if t_r is small enough.

The following special modulation function,

$$f(t) = \begin{cases} P_1, & t \leqslant 0, \\ P_1 + \frac{P_2-P_1}{t_r}t, & 0 < t \leqslant t_r, \\ P_2, & t > t_r, \end{cases} \tag{14}$$

will be used in the next section to fit our experimental results. For the above special modulation function, according to the

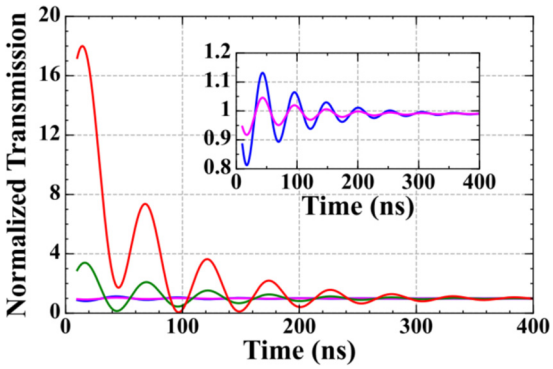

FIG. 2. Relation between $T(t)$ and P_1/P_2 without modal coupling. The values of P_1/P_2 for the blue, magenta, green, and red curves are 0, 0.6, 10, and 35, respectively. The inset is an enlarged view of the blue and magenta curves. Other parameters are $\kappa_e/2\pi = 1.11$ MHz, $\kappa_o/2\pi = 0.80$ MHz, $t_r = 10$ ns, and $\delta/2\pi = 19.10$ MHz.

definition of the parameter α in Eq. (8), there is

$$\alpha = \left(1 - \frac{P_1}{P_2}\right)\frac{1 - e^{(j\delta-\kappa)t_r}}{(-j\delta+\kappa)t_r}. \tag{15}$$

It can be found that when the value of P_1/P_2 is increased from zero, the value of $|\alpha|$ will first decrease to zero and then increase, which means P_1/P_2 can control the amplitude of the second term of $T(t)$ in Eq. (12). In Fig. 2 we demonstrate how the normalized transmission $T(t)$ changes with the value of P_1/P_2 when other parameters are fixed. From Fig. 2 it can be found that when the value of P_1/P_2 is large enough (the red curve), the result is similar to CRDS but it still contains the information on the frequency of the microresonator.

C. Modified CRUS with modal coupling

Assume the coupling strength between the CCW mode E_1 and its corresponding degenerate clockwise (CW) mode E_2 is β. The evolution of the two modes will satisfy the following equations [37],

$$\frac{dE_1(t)}{dt} = (-j\omega_c - \kappa)E_1(t) + j\beta E_2(t) + \sqrt{2\kappa_e}E_{\text{in}}(t), \tag{16}$$

$$\frac{dE_2(t)}{dt} = (-j\omega_c - \kappa)E_2(t) + j\beta E_1(t). \tag{17}$$

These two coupled equations can be decoupled by introducing

$$E_+(t) = E_1(t) + E_2(t), \tag{18}$$

$$E_-(t) = E_1(t) - E_2(t), \tag{19}$$

which satisfy the decoupled equations

$$\frac{dE_+(t)}{dt} = (-j\omega_c - \kappa + j\beta)E_+(t) + \sqrt{2\kappa_e}E_{\text{in}}(t), \tag{20}$$

$$\frac{dE_-(t)}{dt} = (-j\omega_c - \kappa - j\beta)E_-(t) + \sqrt{2\kappa_e}E_{\text{in}}(t). \tag{21}$$

According to the discussion for modified CRUS without modal coupling, the two decoupled equations lead to

$$E_+(t) = \frac{\sqrt{2\kappa_e}}{-j\delta_+ + \kappa}[1 - e^{(j\delta_+-\kappa)(t-t_r)}\alpha_+]E_{\text{in}}(t), \tag{22}$$

$$E_-(t) = \frac{\sqrt{2\kappa_e}}{-j\delta_- + \kappa}[1 - e^{(j\delta_--\kappa)(t-t_r)}\alpha_-]E_{\text{in}}(t), \tag{23}$$

where $t > t_r$, $\delta_+ = \omega_l - \omega_c + \beta$, $\delta_- = \omega_l - \omega_c - \beta$, and

$$\alpha_+ = \frac{1}{P_2}\int_0^{t_r}\frac{df(t')}{dt'}e^{(-j\delta_++\kappa)(t'-t_r)}dt', \tag{24}$$

$$\alpha_- = \frac{1}{P_2}\int_0^{t_r}\frac{df(t')}{dt'}e^{(-j\delta_-+\kappa)(t'-t_r)}dt'. \tag{25}$$

According to the expression of E_{out} in Eq. (3) and the definition of the normalized transmission $T(t)$ in Eq. (11), we can get

$$T(t) = |1 - A_+e^{(j\delta_+-\kappa)\Delta t} - A_-e^{(j\delta_--\kappa)\Delta t}|^2, \tag{26}$$

where $\Delta t = t - t_r > 0$ and

$$A_+ = \frac{\kappa_e}{j\delta_+ - \kappa_o + \frac{-j\delta_++\kappa}{-j\delta_-+\kappa}\kappa_e}\alpha_+, \tag{27}$$

$$A_- = \frac{\kappa_e}{j\delta_- - \kappa_o + \frac{-j\delta_-+\kappa}{-j\delta_++\kappa}\kappa_e}\alpha_-. \tag{28}$$

We note that the modulation function $f(t)$ in Eq. (14) will be used in the next section to fit our experimental results with modal coupling, which leads to

$$\alpha_+ = \left(1 - \frac{P_1}{P_2}\right)\frac{1 - e^{(j\delta_+-\kappa)t_r}}{(-j\delta_++\kappa)t_r}, \tag{29}$$

$$\alpha_- = \left(1 - \frac{P_1}{P_2}\right)\frac{1 - e^{(j\delta_--\kappa)t_r}}{(-j\delta_-+\kappa)t_r}. \tag{30}$$

The normalized transmission $T(t)$ in Eq. (26) describes the interference of three terms, which contains information about frequency, decay rate, and coupling strength between the degenerate CW and CCW modes. This is very clear under the following special conditions. When the laser detuning δ is so large and its amplitude changing time t_r is so small that

$$\beta \ll |\delta|, \quad \kappa \ll |\delta|, \quad |\delta t_r| \ll 1, \tag{31}$$

this will lead to

$$A_+ \approx A_- \approx A = \frac{-j\kappa_e}{\delta}\left(1 - \frac{P_1}{P_2}\right). \tag{32}$$

We emphasize that the above approximation is applicable for a general modulation function $f(t)$. Additionally if there is $|A| \ll 1$, the normalized transmission $T(t)$ in Eq. (26) can be approximately by

$$T(t) \approx 1 - \frac{4\kappa_e}{\delta}\left[1 - \frac{P_1}{P_2}\right]e^{-\kappa\Delta t}\sin(\delta\Delta t)\cos(\beta\Delta t), \tag{33}$$

where terms proportional to $|A|^2$ are ignored. As $\beta \ll |\delta|$ in the above, δ is a fast frequency and β is a slowly beat frequency. Figure 3 gives a graphical demonstration of $T(t)$ in Eq. (33) where δ, β, and κ are marked.

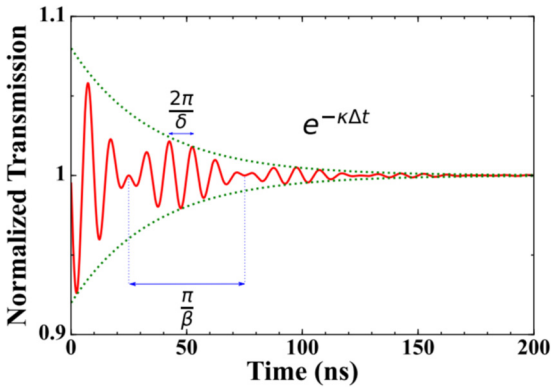

FIG. 3. A graphical demonstration of $T(t)$ with modal coupling in Eq. (33). The curve is draw with parameters $\kappa_e/2\pi = 2.00$ MHz, $\kappa_o/2\pi = 2.50$ MHz, $\delta/2\pi = 100.00$ MHz, $\beta/2\pi = 10.00$ MHz, $P_1/P_2 = 0$, and $t_r = 0.1$ ns, respectively.

III. EXPERIMENTS OF MODIFIED CRUS

Our experimental setup of modified CRUS is shown in Fig. 4. A fiber taper is used to couple light into and out of a silica microsphere which is made by melting a single-mode fiber tip using a CO_2 laser. The fiber taper is made by using a motorized translational stage to stretch a single-mode fiber from its two ends and simultaneously being heated by a hydrogen flame. The fabricated fiber taper has a diameter of about 2 μm and the diameter of the microsphere is about 160 μm. A wavelength-tunable laser (Newport TLB-6700) provides a monochromatic light with a wavelength of about 1545 nm. The laser intensity is modulated by an electric-optical modulator (EOM) (Thorlabs model LN81S-FC), which is input a square-wave electric signal with a period of 2000 ns from an arbitrary function generator (AFG). The low and high voltages of the square-wave electric signal are used to control the value of P_1/P_2 in the theory. The laser from the output of the EOM is linked to a circulator which combined with the photodetector PD2 in Fig. 4 is used to detect whether there exists a reflected light. A strong reflected light means that the coupling between the CW and CCW modes of the microsphere cannot be ignored. A high-speed photodetector (PD1 in Fig. 4) (Newport model 818-BB-35F) is used to measure the light out of the fiber taper. Before the high-speed photodetector there is an erbium-doped fiber amplifier (Thorlabs EDFA100S) and a tunable bandpass filter (Newport TBF-1550-1.0-FCAPC),

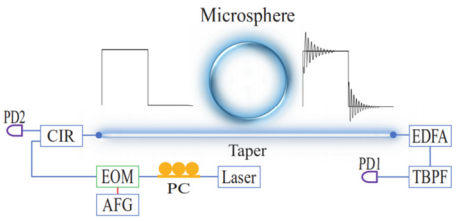

FIG. 4. Schematic diagram of the experimental setup. PC1: polarization controller; EOM: electric-optical modulator; AFG: arbitrary function generator; CIR: circulator; EDFA: erbium-doped fiber amplifier; TBPF: tunable bandpass filter; PD1: high-speed fiber photodetector; PD2: low-noise photodetector.

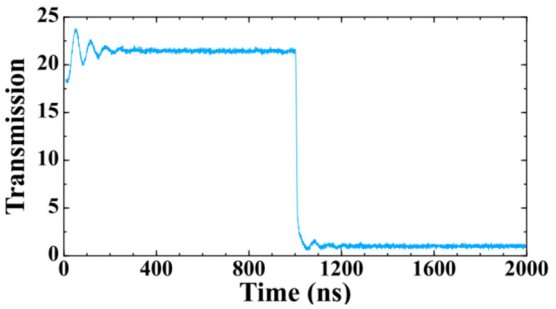

FIG. 5. Two experimentally observed modified CRUS in one period. The final value of the transmission is normalized to the unit.

which are used to improve the signal-to-noise ratio. The fiber taper and the microsphere are fixed on nanostages with a resolution of 20 nm (Thorlabs MAX312D), so that we can control the gap between them.

In our experiment, the intensity of the laser into the fiber taper is switched between a small value and a large value periodically and its one period is shown in Fig. 4, where the rising edge corresponds to theory with $P_1 < P_2$ and the falling edge corresponds to theory with $P_1 > P_2$, respectively. Therefore the measurement in one period can record two related modified CRUS, i.e., one has $P_1/P_2 = P_0 < 1$ and the other has $P_1'/P_2' = P_0' = 1/P_0 > 1$. In Fig. 5 two experimentally observed related modified CRUS in one period are presented. We note that the modified CRUS with a large P_1/P_2 is similar to CRDS as shown in Fig. 2, but a large P_1/P_2 is not easy to be achieved in our experiment. This is because in experiment P_1 cannot be too large for avoiding the thermal effect of the microsphere, and P_2 cannot be too small as the noise of the high-speed photodetector is high.

We have done two groups of experiments, one without modal coupling and the other with the coupling between the CW and CCW modes. The first group of experimental results without modal coupling is shown in Fig. 6, and the second group of experimental results with modal coupling is shown in Fig. 7. In each group of experiments, we try to keep the system stable and only change the value of P_1/P_2 to observe its influence on the oscillation amplitude of the normalized transmission $T(t)$. Two subfigures in each row of Fig. 6 (Fig. 7) are recorded in the same period as that in Fig. 5, and they are fitted with the same parameters except for P_1/P_2 (the fitting values of P_1/P_2 for two subfigures on the same row have a reciprocal relationship). The experimental results demonstrate that the value of P_1/P_2 can affect the oscillation amplitude of $T(t)$. It can be found that the values of κ_e and δ in Fig. 6 (Fig. 7) are not the same for all subfigures, which should be the same if the experiments were perfect. This is because there is some instability in the system. The parameter κ_e can be affected by the gap between the fiber taper and the microsphere, and the parameter δ can be affected by the wavelength shift of the laser and the thermal effect of the microsphere. We note that in the theoretical fittings the laser amplitude modification function $f(t)$ in Eq. (14) is used.

In the theoretical discussion of the modified CRUS with modal coupling, it has been shown that if the conditions in Eq. (31), i.e., $\beta \ll |\delta|$, $\kappa \ll |\delta|$, and $|\delta t_r| \ll 1$, are satisfied,

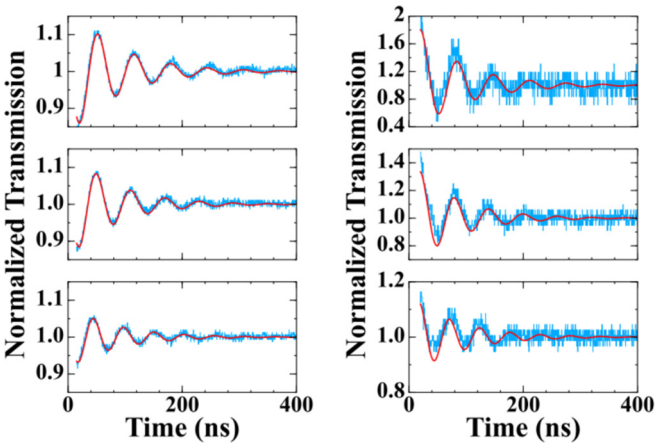

FIG. 6. Experimental modified CRUS without modal coupling. The data on the left column are fitted with P_1/P_2 being 0.21, 0.40, and 0.57 from top to bottom, $\kappa_e/2\pi$ being 0.91, 1.04, and 0.95 MHz from top to bottom, $\delta/2\pi$ being 15.70, 16.65, and 18.89 MHz from top to bottom, and unchanged parameters $\kappa_o/2\pi = 1.00$ MHz, $t_r = 10$ ns. The data on the right column and the corresponding data on the left column in the same row are fitted with the same parameters except for P_1/P_2 as they are recorded in one period.

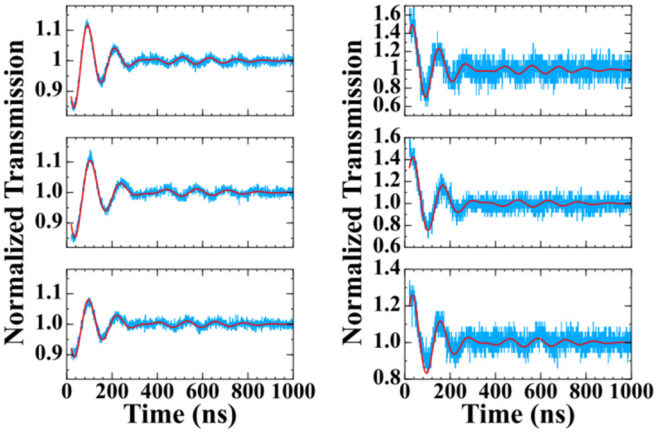

FIG. 7. Experimentally modified CRUS with coupling between the CW and CCW modes. The data on the left column are fitted with P_1/P_2 being 0.29, 0.38, and 0.45 from top to bottom, $\kappa_e/2\pi$ being 0.55 , 0.54, and 0.46 MHz from top to bottom, $\delta/2\pi$ being 8.37, 7.42, and 8.03 MHz from top to bottom, and unchanged parameters $\kappa_o/2\pi = 0.18$ MHz, $t_r = 10$ ns, and $\beta/2\pi = 0.72$ MHz. The data on the right column and the corresponding data on the left column in the same row are fitted with the same parameters except for P_1/P_2 as they are recorded in one period.

an approximate expression of the normalized transmission $T(t)$ in Eq. (33) will be obtained, where the meanings of δ, β, and κ are very clear. From the values of the fitting parameters given in the caption of Fig. 7, it can be found that $\beta \ll |\delta|$ and $\kappa \ll |\delta|$ are satisfied, but the value of $|\delta t_r|$ is about 0.5 and is not much smaller than one. In our experiment, the value of t_r is 10 ns, which can be less than 1 ns to satisfy the condition $|\delta t_r| \ll 1$ if a more sophisticated AFG is used. So the conditions in Eq. (31) can be experimentally achieved.

IV. DISCUSSION AND SUMMARY

That CRUS can be used to sense ultrafast phenomena is based on the fact that we can record a CRUS within a very short time. The timescale of ultrafast phenomena that can be sensed by CRUS depends on the time needed to record a CRUS, which has a relation to the decay rate κ of the WGM mode. In the original CRUS [28], the period of the square-wave signal used to control the laser intensity should be larger than $2/\kappa$, and only one CRUS can be recorded in a single period. However, in our protocol two modified CRUS can be recorded in a single period of the square-wave signal (see Fig. 5), which reduces the time to record a CRUS and thus is an advantage for sensing ultrafast phenomena.

In summary, we give the theory of a modified CRUS and present its experimental observation. Theoretically, an explicit dependence of the modified CRUS on the laser amplitude modification function $f(t)$ has been obtained. Experimentally, how to observe modified CRUS in the experiment is given in detail, and experiments of the modified CRUS with and without modal coupling are both presented. CRUS provides a method to sense ultrafast phenomena that extends the application of WGM microresonators, and it is still in developing [28–30]. The results in this paper enrich our knowledge about CRUS.

ACKNOWLEDGMENTS

This work was supported by the National Natural Science Foundation of China (Grants No. 12074067 and No. 11674059), and the Natural Science Foundation of Fujian Province of China (Grant No. 2020J01191).

[1] T. Kippenberg and K. Vahala, Cavity opto-mechanics, Opt. Express **15**, 17172 (2007).

[2] Z. Shen, Y.-L. Zhang, Y. Chen, C.-L. Zou, Y.-F. Xiao, X.-B. Zou, F.-W. Sun, G.-C. Guo, and C.-H. Dong, Experimental realization of optomechanically induced non-reciprocity, Nat. Photonics **10**, 657 (2016).

[3] G. Wang, M. Zhao, Y. Qin, Z. Yin, X. Jiang, and M. Xiao, Demonstration of an ultra-low-threshold phonon laser with coupled microtoroid resonators in vacuum, Photonics Res. **5**, 73 (2017).

[4] Q.-T. Cao, R. Liu, H. Wang, Y.-K. Lu, C.-W. Qiu, S. Rotter, Q. Gong, and Y.-F. Xiao, Reconfigurable symmetry-broken laser in a symmetric microcavity, Nat. Commun. **11**, 1136 (2020).

[5] J. Li, S. Zhang, R. Yu, D. Zhang, and Y. Wu, Enhanced optical nonlinearity and fiber-optical frequency comb controlled by a single atom in a whispering-gallery-mode microtoroid resonator, Phys. Rev. A **90**, 053832 (2014).

[6] Y.-S. Park, A. K. Cook, and H. Wang, Cavity QED with diamond nanocrystals and silica microspheres, Nano Lett. **6**, 2075 (2006).

[7] Z. Shen, Y.-L. Zhang, C.-L. Zou, G.-C. Guo, and C.-H. Dong, Dissipatively Controlled Optomechanical Interaction via Cascaded Photon-Phonon Coupling, Phys. Rev. Lett. **126**, 163604 (2021).

[8] Y. Chen, Y.-L. Zhang, Z. Shen, C.-L. Zou, G.-C. Guo, and C.-H. Dong, Synthetic Gauge Fields in a Single Optomechanical Resonator, Phys. Rev. Lett. **126**, 123603 (2021).

[9] J. Zhang, B. Peng, S. Kim, F. Monifi, X. Jiang, Y. Li, P. Yu, L. Liu, Y.-x. Liu, A. Alù, and L. Yang, Optomechanical dissipative solitons, Nature (London) **600**, 75 (2021).

[10] Q. Song, Emerging opportunities for ultra-high Q whispering gallery mode microcavities, Sci. China: Phys., Mech. Astron. **62**, 74231 (2019).

[11] J.-h. Chen, X. Shen, S.-J. Tang, Q.-T. Cao, Q. Gong, and Y.-F. Xiao, Microcavity Nonlinear Optics with an Organically Functionalized Surface, Phys. Rev. Lett. **123**, 173902 (2019).

[12] Y. Hu, S. Ding, Y. Qin, J. Gu, W. Wan, M. Xiao, and X. Jiang, Generation of Optical Frequency Comb via Giant Optomechanical Oscillation, Phys. Rev. Lett. **127**, 134301 (2021).

[13] S. Zhu, W. Wang, B. Jiang, L. Ren, L. Shi, and X. Zhang, Flexible manipulation of lasing modes in an erbium-doped microcavity via an add–drop configuration, ACS Photonics **8**, 3069 (2021).

[14] Y. Bai, M. Zhang, Q. Shi, S. Ding, Y. Qin, Z. Xie, X. Jiang, and M. Xiao, Brillouin-Kerr Soliton Frequency Combs in an Optical Microresonator, Phys. Rev. Lett. **126**, 063901 (2021).

[15] W. Wang, L. Wang, and W. Zhang, Advances in soliton microcomb generation, Adv. Photonics **2**, 034001 (2020).

[16] Z. Guo, Y. Qin, P. Chen, J. Hu, Y. Zhou, X. Zhao, Z. Liu, Y. Fei, X. Jiang, and X. Wu, Hyperboloid-drum microdisk laser biosensors for ultrasensitive detection of human IgG, Small **16**, 2000239 (2020).

[17] Z. Shen, Y.-L. Zhang, Y. Chen, F.-W. Sun, X.-B. Zou, G.-C. Guo, C.-L. Zou, and C.-H. Dong, Reconfigurable optomechanical circulator and directional amplifier, Nat. Commun. **9**, 1797 (2018).

[18] H.-J. Chen, Q.-X. Ji, H. Wang, Q.-F. Yang, Q.-T. Cao, Q. Gong, X. Yi, and Y.-F. Xiao, Chaos-assisted two-octave-spanning microcombs, Nat. Commun. **11**, 2336 (2020).

[19] E. Kim, M. D. Baaske, and F. Vollmer, Towards next-generation label-free biosensors: Recent advances in whispering gallery mode sensors, Lab Chip **17**, 1190 (2017).

[20] Y. Zhi, X.-C. Yu, Q. Gong, L. Yang, and Y.-F. Xiao, Single nanoparticle detection using optical microcavities, Adv. Mater. **29**, 1604920 (2017).

[21] G. C. Righini and S. Soria, Biosensing by WGM microspherical resonators, Sensors **16**, 905 (2016).

[22] L. He, Ş. K. Özdemir, J. Zhu, W. Kim, and L. Yang, Detecting single viruses and nanoparticles using whispering gallery microlasers, Nat. Nanotechnol. **6**, 428 (2011).

[23] J. C. Knight, G. Cheung, F. Jacques, and T. A. Birks, Phase-matched excitation of whispering-gallery-mode resonances by a fiber taper, Opt. Lett. **22**, 1129 (1997).

[24] P. Chang, B. Cao, F. Gao, L. Huang, W. Zhang, F. Bo, X. Yu, G. Zhang, and J. Xu, Enhance stable coupling region of a high-Q WGM up to micrometer, Appl. Phys. Lett. **115**, 211104 (2019).

[25] F. Vollmer and S. Arnold, Whispering-gallery-mode biosensing: Label-free detection down to single molecules, Nat. Methods **5**, 591 (2008).

[26] J. Zhu, S. K. Ozdemir, Y.-F. Xiao, L. Li, L. He, D.-R. Chen, and L. Yang, On-chip single nanoparticle detection and sizing by mode splitting in an ultrahigh-Q microresonator, Nat. Photonics **4**, 46 (2010).

[27] L. Shao, X.-F. Jiang, X.-C. Yu, B.-B. Li, W. R. Clements, F. Vollmer, W. Wang, Y.-F. Xiao, and Q. Gong, Detection of single nanoparticles and lentiviruses using microcavity resonance broadening, Adv. Mater. **25**, 5616 (2013).

[28] S. Rosenblum, Y. Lovsky, L. Arazi, F. Vollmer, and B. Dayan, Cavity ring-up spectroscopy for ultrafast sensing with optical microresonators, Nat. Commun. **6**, 6788 (2015).

[29] Y. Yang, R. Madugani, S. Kasumie, J. M. Ward, and S. Nic Chormaic, Cavity ring-up spectroscopy for dissipative and dispersive sensing in a whispering gallery mode resonator, Appl. Phys. B **122**, 291 (2016).

[30] M.-Y. Ye and X.-M. Lin, Theory of cavity ring-up spectroscopy, Opt. Express **25**, 32395 (2017).

[31] F.-J. Shu, C.-L. Zou, Şahin Kaya Özdemir, L. Yang, and G.-C. Guo, Transient microcavity sensor, Opt. Express **23**, 30067 (2015).

[32] M.-Y. Ye, M.-X. Shen, and X.-M. Lin, Ringing phenomenon based whispering-gallery-mode sensing, Sci. Rep. **6**, 19597 (2016).

[33] S. Trebaol, Y. Dumeige, and P. Féron, Ringing phenomenon in coupled cavities: Application to modal coupling in whispering-gallery-mode resonators, Phys. Rev. A **81**, 043828 (2010).

[34] A. O'Keefe and D. A. G. Deacon, Cavity ring-down optical spectrometer for absorption measurements using pulsed laser sources, Rev. Sci. Instrum. **59**, 2544 (1988).

[35] A. A. Savchenkov, A. B. Matsko, V. S. Ilchenko, and L. Maleki, Optical resonators with ten million finesse, Opt. Express **15**, 6768 (2007).

[36] G. C. Righini, Y. Dumeige, P. Féron, M. Ferrari, G. Nunzi Conti, D. Ristic, and S. Soria, Whispering gallery mode microresonators: Fundamentals and applications, Riv. Nuovo Cimento **34**, 435 (2011).

[37] T. J. Kippenberg, S. M. Spillane, and K. J. Vahala, Modal coupling in traveling-wave resonators, Opt. Lett. **27**, 1669 (2002).